Journal of Applied Mechanics and Technical Physics, Vol. 42, No. 5, pp. 857–863, 2001

THIRD HEAT-TRANSFER CRISIS WITH STEPWISE HEAT SUPPLY

B. P. Avksentyuk and V. V. Ovchinnikov

UDC 536.248

The paper reports experimental results on heat-transfer crises with stepwise heat supply to a heater, in which the metastable liquid decomposes in the form of vaporization fronts. Data on the dynamics of heat-transfer crises under saturation and underheating conditions are given. It is shown that below the vapor formed during propagation of vaporization fronts, a liquid microlayer is absent.

Introduction. Transient processes during boiling, including heat-transfer crises, are of considerable interest because the heating surfaces of modern energy-intensive apparatus need stable cooling during local thermal perturbations of its elements. During bubble boiling, heat removal remains highly intense only until certain heat-flux densities, above which the contact of the liquid with the thermally stressed surface breaks, which leads to an abrupt decrease in heat transfer (crisis). Trouble-free operation of devices with liquid heat carriers is largely determined by a proper choice of operation conditions, which prevents heat-transfer crises.

Previous studies [1–3] of the boiling of alkali metals and organic liquids under free convection with quasisteady-state heat supply to a heat-transfer surface revealed a new type of heat-transfer crisis, in which the transition from single-phase convection to film boiling is due to propagation of vaporization fronts. This type of boiling process was called a "third heat-transfer crisis." It was shown that the heat-flux densities leading to a third heat-transfer crisis can be much lower than the critical heat-flux densities for bubble boiling $q_{\rm cr,1}$. The range of regime parameters in which this type of crisis can occur under free convection conditions was determined [1, 2, 4, 5]. However, experiments on a third heat-transfer crises under conditions of unsteady heat supply have not been performed.

Experimental studies of transient heat transfer (including crises) are rather extensive (see, e.g., [6–10]). Our results on heat-transfer crises with stepwise heat supply to a heater show that the wall metastable liquid decomposes to form vaporization fronts. Data on the dynamics of heat-transfer crises under saturation and underheating conditions are given.

Measuring Method. Experiments were performed with KhCh toluene in a large volume of an undisturbed liquid. The working section was made of a platinum wire 68 mm long and 100 μm in diameter which was soldered to copper rods of 10 mm diameter. The working section was placed horizontally in the working volume. The liquid level above the working section was 65 mm. To measure the gas and liquid temperatures in the working volume, we placed thermocouples in the liquid at the level of the working section and in the vapor region.

The working volume was heated by passage of an electric current through the working section, to which a stepwise voltage pulse was applied with a rate of pulse rise of the order of 10^4 V/sec. Electric pulse parameters were specified by supply voltage control with an electronic voltage stabilizer. The control system operated with a frequency of 50 kHz, which ensured high reliability. The working section was also used as a resistance thermometer. The dependence of the electric resistance of the working section on temperature was measured previously under steady-state conditions.

An acoustic pressure sensor was placed in the working volume record the onset of vaporization. Prior to a power surge, we measured the pressures and temperatures of the liquid and vapor in the working volume. Measurements under unsteady conditions were performed using a computerized, programmable, two-channel, 12-digit, analog-to-digital converter with a time resolution of 11.2 μsec per channel.

Kutateladze Institute of Thermal Physics, Siberian Division, Russian Academy of Sciences, Novosibirsk 630090. Translated from Prikladnaya Mekhanika i Tekhnicheskaya Fizika, Vol. 42, No. 5, pp. 143–151, September–October, 2001. Original article submitted August 16, 2000; revision submitted February 19, 2001.

0021-8944/01/4205-0857 $25.00 © 2001 Plenum Publishing Corporation

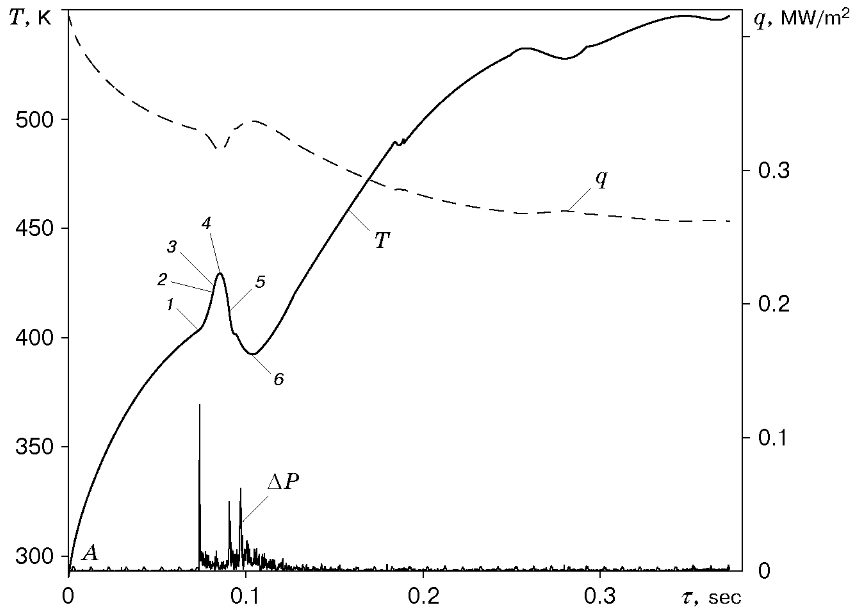

Fig. 1

Voltage supply to the working section, sensor polling, determination of the boiling point, and provision of time necessary for measurements before and after boiling were performed by an automated control equipment governed by a special program. The electric resistance and electric power released in the working section were determined from current and voltage measurements. The average temperature of the working section was determined from the temperature curve of electric resistance. The vaporization process in the working section was video recorded.

In the experiments, the toluene pressures in the working volume was varied from 1.7 to 75 kPa, and the liquid was heated to a temperature 3–82 K below the saturation temperature. The saturation temperature in the vicinity of the heat-transfer surface was determined with allowance for the weight of the liquid column. Underheating of the liquid was obtained by addition of air into the working volume.

The time dependences of the average temperature of the working section and the power released in the working section for various values of power surge were approximated by piecewise-smooth functions (the mean-square approximation error corresponded to the measurement error). These functions were used to calculate integral-averaged (over the heat-transfer surface) values of the heat flux removed from the working section at various times by the formula

$$q_1(\tau) = q(\tau) - 0.25\, d\rho c_p\, \frac{dT(\tau)}{d\tau},$$

where q is the heat-generation rate in the working section, τ is time, T is the average temperature of the working section, and d, c_p, and ρ are, respectively, the diameter, heat capacity, and density of the working section.

Experimental Results. Video-recording data showed that in all experiments, when a heat-transfer crisis arouse upon heat-power surge, vaporization in the metastable liquid occurred in the form of vaporization fronts.

Experiments were conducted under saturation conditions at a working pressure of $P = 2.3$–2.7 kPa. Figures 1 and 2 show experimental data illustrating the dynamics of a heat-transfer crisis under saturation conditions. Figure 1 shows a curve of the average temperature of the working section versus time for an initial heat-generation rate of $q_0 = 0.42$ MW/m^2. The pressure P in the working volume was 2.6 kPa, and the underheating of the liquid relative to the saturation temperature ΔT_{sub} due to the weight of the liquid column was 4.2 K. Figure 1 also shows values of the heat-transfer rates in the working section and the pressure pulse ΔP that arouse in the acoustic pressure sensor during boiling. Solid curve in Fig. 2 shows the heat flux removed from the surface of the working section versus the superheat of the working section ΔT_s relative to the saturation temperature. The arrows show the direction of variation in q_l with time. Data obtained under quasisteady-state heating (dashed curves) are given in this figure for comparison: the curve ACB corresponds to single-phase convection in the liquid, the curve CD corresponds to bubble boiling, and the curve EF corresponds to film boiling. The point D corresponds to the first critical heat flux.

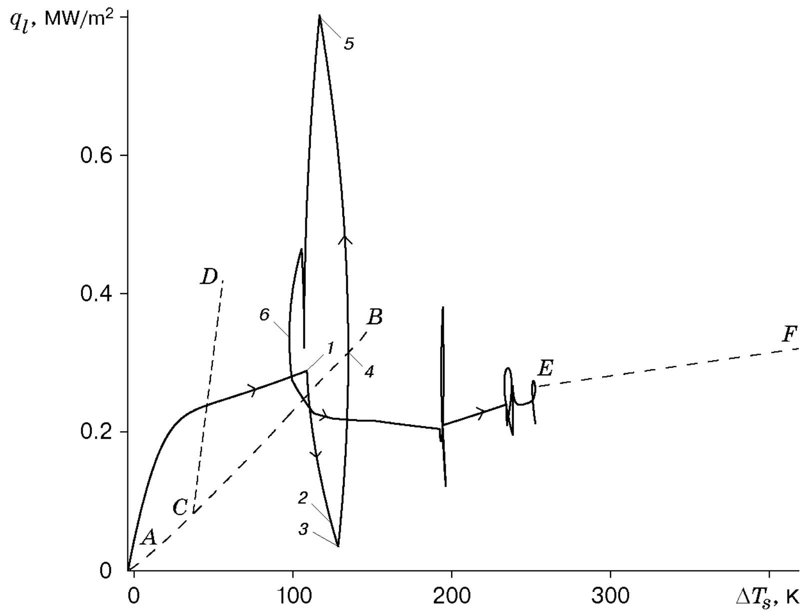

Fig. 2

After a power surge, heat was transferred from the working section by heat conduction (curves A1 in Figs. 1 and 2). The liquid boiled up 73.5 msec after the power surge at a superheat temperature of 108.6 K (points 1 in Figs. 1 and 2). At that moment, the heat flux transferred to the liquid was 0.29 MW/m^2. A bubble formed at a distance of 11 mm from the edge of the working section. In this experiment, the propagation velocity of the vaporization front was 7.7 m/sec. Vaporization fronts spread over the entire heat-transfer surface in 7.4 msec (points 2). After boiling, the amplitude of the acoustic signal and the growth rate of heater's temperature increased, and the heat flux removed from the heater began decreasing.

After the vaporization fronts had spread over the entire heat-transfer surface, the temperature of the heater continued increasing, and the amplitude of the acoustic signal decreased. The removed heat flux decreased to 0.034 MW/m^2 at $\tau_b = 8.6$ msec (points 3 in Figs. 1 and 2), and the working section temperature increased to 429 K at $\tau_b = 12$ msec (points 4) ($\tau_{\rm b}$ is the elapsed time from the moment of boiling). Then, at $\tau_{\rm b} = 17.2$ msec (points 5) the removed heat flux increased to 0.8 MW/m^2, which is much larger than the value of $q_{{\rm cr},1}$, and the temperature of the working section decreased to 392 K at $\tau_{\rm b} = 30$ msec (points 6). The process was accompanied by an increase in the amplitude of the acoustic signal. Simultaneously, partial failure, deformation, and separation of the vapor formation from the heat-transfer surface were observed. At the next stage of the experiment, the working section temperature reached a value corresponding to steady-state film boiling.

Under saturation conditions, the superheat temperature prior to boiling exceeded 100 K, and a heat-transfer crisis occurred. After supply of low-density heat fluxes, the liquid did not boil, and single-phase free convection occurred on the heater. To obtain lower values of superheat prior to boiling, we used the following experimental procedure: after supply of heat power sufficient for vaporization, the liquid boiled, and after 50 msec, the heat load was cut off. Then, after 200 msec, a new supply of lower heat power was performed. This provided low superheat values before boiling.

With supply of heat fluxes equal to $0.8q_{{\rm cr},1}$ and superheat temperatures before boiling below 64 K, unsteady film boiling was observed on the heat-transfer surface. In the range of $\Delta T_s = 64$–72 K, bubble boiling or film boiling could occur. At higher superheat prior to boiling, a heat-transfer crisis always took place.

When the liquid was underheated with respect to the saturation temperature, propagation of condensation fronts along with vaporization fronts was observed [11]. Figure 3 shows time variations in the average temperature of the working section, pressure pulse, and released power at $q_0 = 0.77$ MW/m^2, $P = 13.1$ kPa, and $\Delta T_{\rm sub} = 32.6$ K. Figure 4 shows a curve of q_l versus superheat under the same conditions (thick curve). The notation on the dashed curves (quasisteady-state conditions) is the same as in Fig. 2. The liquid boiled up within 90.8 msec after a power surge at a superheat temperature of 167 K (points 1 in Figs. 3 and 4). A bubble formed at a distance of 24 mm

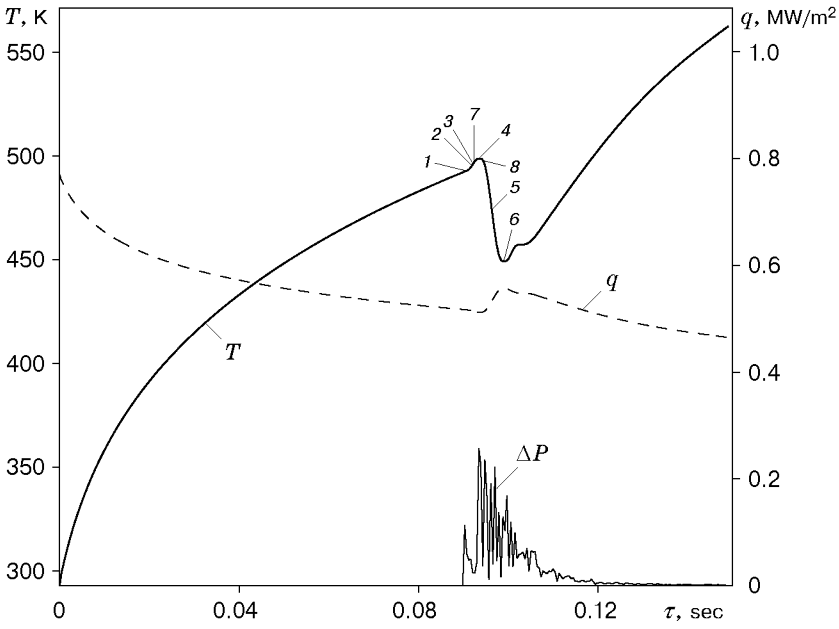

Fig. 3

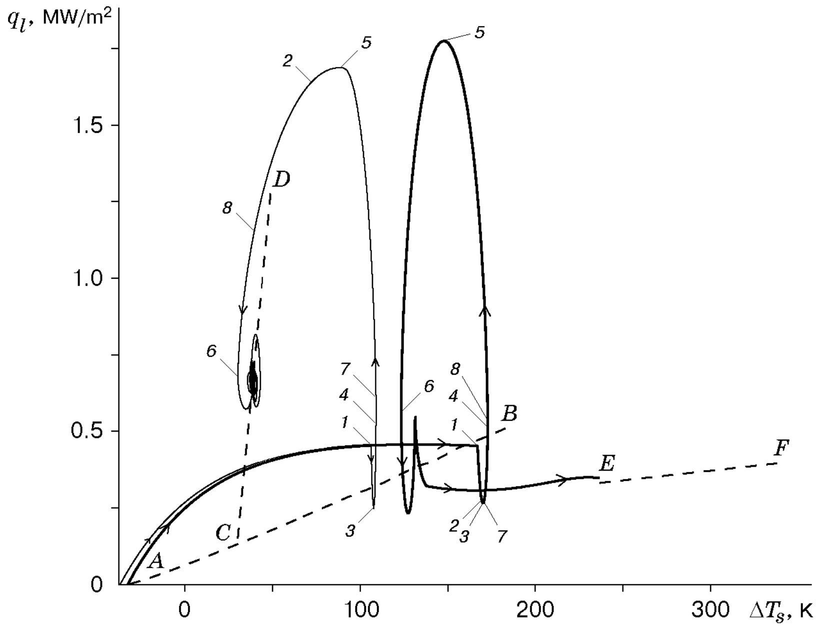

Fig. 4

from the edge of the working section. The propagation velocity of the vaporization front was 29.5 m/sec. In a time of $\tau_{\mathrm{b}} = 1.4$ msec, the vaporization fronts spread over the entire heat-transfer surface (points 2).

As in the experiments under saturation conditions, after boiling, the growth rate of the temperature of the heater increased; the heat flux removed from the heater began decreasing, and within 1.54 msec it reached the minimum value of 0.26 MW/m^2 (points 3) after which it began increasing again. At $\tau_{\mathrm{b}} = 1.1$ msec, the cross-sectional dimension of the vapor formation at the site of bubble initiation began decreasing. Condensation fronts formed within 1.5 msec after boiling (points 7) and propagated over the heat-transfer surface during roughly 1.6 msec (points 8). The working section temperature reached the maximum value of 499 K at $\tau_{\mathrm{b}} = 3.1$ msec (point 4). After this, it decreased to 449 K at $\tau_{\mathrm{b}} = 8.47$ msec (points 6), and the removed heat flux increased to 1.78 MW/m^2 at $\tau_{\mathrm{b}} = 5.78$ msec (points 5). Ultimately, the temperature of the heater increased again to a value corresponding to steady-state film boiling.

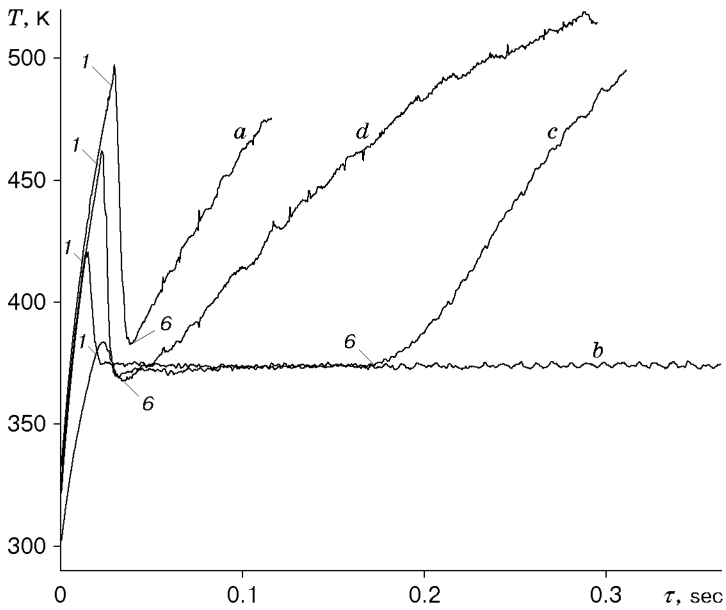

Fig. 5

Figure 4 shows experimental results (thin curve) obtained under conditions similar to those described above ($q_0 = 0.79$ MW/m^2, $P = 13.8$ kPa, and $\Delta T_{\rm sub} = 37.2$ K). The experimental conditions differed in that the superheat temperature prior to boiling was substantially lower ($\Delta T_s = 106$ K) and the bubble boiling regime was established on the heater after boiling up. The propagation velocity of the vaporization front was 12 m/sec. Condensation fronts formed 1.2 msec after boiling up. Their propagation velocities were 8 m/sec. In the bubble boiling regime, pulsations of the temperature of the working section were observed, which were due to the formation of bubbles. Therefore, the pathway corresponding to film boiling was a loop rotating anticlockwise around the point ($\Delta T_{\rm st} = 38.7$ K and $q_{\rm st} = 0.66$ MW/m^2) on the curve of steady-state bubble boiling.

Under underheating conditions, the development of heat-transfer crises had the following special feature: the time from boiling to the moment of formation of a stable vapor film, when the temperature increased to a value corresponding to steady-state film boiling, could change significantly (from ten to hundreds of milliseconds) even if the heat fluxes supplied to the working section were identical.

Curves a, b, and c shown in Fig. 5 were obtained at the same initial heat-generation rate equal to 1.19 MW/m^2 ($\Delta T_{\rm sub} = 36$ K and $P = 13$ kPa). As can be seen from Fig. 5, after boiling, the heat-transfer process follows various pathways. At the highest superheat temperatures prior to boiling $\Delta T_s = 164$ K (curve a in Fig. 5), the working section temperature decreased to a value higher than the value corresponding to the steady-state bubble boiling curve. In this experiment, the time of crisis development from the boiling point (point 1) till the onset of temperature rise (point 6) was 12.4 msec.

At a superheat of 131 K prior to boiling (curve b), the working section temperature decreased to a value lower than that corresponding to bubble boiling. Then, after 10 msec, the temperature increased to the bubble boiling temperature and remained constant for 350 msec until the loading was cut off. At a lower superheat of 95 K prior to boiling (curve c), the temperature of the working section decreased to the temperature of bubble boiling and remained unchanged during 154 msec. Then, it started decreasing monotonically with a rate of roughly 900 K/sec, which indicated that a heat-transfer crisis occurred.

Figure 5 shows the data obtained at $q_0 = 0.69$ MW/m^2, $\Delta T_{\rm sub} = 29.6$ K, and $P = 11.2$ kPa (curve d). Despite the smaller initial heat-generation rate and lower superheat prior to boiling (58 K), a heat-transfer crisis occurred 15 msec after boiling, which was much earlier than in the previous experiment (curve c). Figure 6 shows the time of crisis development versus the initial rate of heat generation in the working section at $\Delta T_{\rm sub} = 28$–35 K and $\Delta T_s = 54$–177 K. At $q_0 < q_{{\rm cr},1}$, a considerable spread of data is observed. At $q_0 > q_{{\rm cr},1}$, the values of $\tau_{\rm cr}$ decrease significantly.

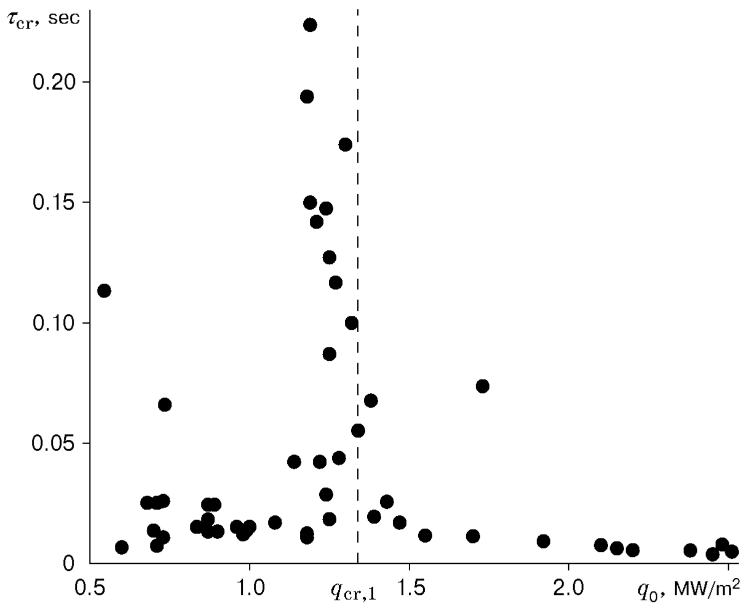

Fig. 6

In some experiments with large underheating (roughly 80 K), the working section temperature decreased to values smaller than the saturation temperature. This showed that heat exchange proceeds with participation of the liquid outside the superheated layer formed by the moment of boiling after a heat power surge.

Discussion of Results. Studies of the dynamics of a third heat-transfer crisis with stepwise heat release in the working section of small diameter under saturation and underheating conditions show that under the vapor formed during propagation of the vaporization front there is no liquid microlayer. Explosive boiling occurs on the heat-transfer surface when the metastable wall liquid decomposes to form propagating vaporization fronts, and the heat transfer from the working section decreases. Although the propagation velocity of the vaporization front is an order of magnitude higher than the liquid-vaporization rate, after passage of the front, a residual liquid layer is either absent on the heat-transfer surface or it is so thin that its vaporization does not affect the dynamics of the working section temperature.

Based on the experimental results presented above, we propose the following mechanism of occurrence of a third heat-transfer crisis under saturation conditions. In a liquid superheated above certain threshold values prior to boiling, instability develops on the surface of a vapor bubble that grows on the heat-transfer surface [12]. This leads to formation of vaporization fronts, which propagate in the wall metastable liquid with a constant (in time) velocity. Their propagation velocity depends strongly on superheat, and at large superheat temperatures, it can reach tens of meters per second.

The vapor produced by propagation of the vaporization fronts isolates the heat-transfer surface from the bulk of the liquid, which results in decrease in heat transfer (section 1–2 of the curves in Figs. 1 and 2). After propagation of the vaporization fronts over the entire heat-transfer surface, the vapor formation continues growing to sizes far exceeding the vapor-film thickness during steady-state film boiling. Therefore, the heat transfer decreases to values well below those observed in steady-state film boiling (section 2–3).

After the stage of expansion, the vapor formation enters a compression stage. On the liquid–vapor interface, perturbations develop due to Taylor instability. The vapor formation partly fails and separates from the working section. Part of the heat-transfer surface is moistened with the liquid. At this stage (section 3–5), the heat transfer increases. The heat flux removed from the working section reaches values far beyond $q_{cr,1}$. Then, in the region of the heat-transfer surface separated from the bulk of the liquid by residues of the vapor formation, there is increase in temperature due to low heat transfer. The vapor film spreads over the entire heat-transfer surface, and steady-state film boiling is established in the working section.

For the underheated liquid, the initial stage of transition to steady-state film boiling is similar to that under saturation conditions: after boiling, vaporization fronts arise, and the heat-transfer surface is isolated from the bulk of the liquid by the vapor produced by propagation of the vaporization fronts. After expansion, the transverse dimensions of the bubble and the adjacent section of the vapor decrease until complete failure. This results in appearance of condensation fronts, which propagate along the surface of the working section with a constant velocity. After passage of the condensation fronts, bubble boiling with underheating is observed on the heat-transfer surface. Initially, this leads to a decrease in the rate of increase in temperature and then to a decrease in the temperature of the working section (section 4–6 of the curves in Figs. 3 and 4).

The experiments show that if the minimum temperature of the working section (point 6 in Fig. 5) is higher than the temperature corresponding to steady-state bubble boiling, the working section temperature increases to the value corresponding to the film boiling regime right after it reaches the minimum. If the temperature of the working section is lower than this value, transition to the steady-state bubble boiling curve is observed, and transition to the film boiling regime can occur after hundreds of milliseconds.

The experimental results for quasisteady-state conditions given in Figs. 2 and 4 are averaged over time and the volume of the working section. In the experiments described above, we measured values averaged over the volume of the working section. Despite averaging, measured values differed greatly from time-averaged values. The difference between local values of heat flux and superheat will be even more significant. The bubble boiling curve plotted using local values of heat-flux density and superheat will be radically different from the steady-state curve. The point $q_l(\Delta T_s)$ rotates anticlockwise around the averaged value corresponding to the steady-state bubble boiling curve, and its path has the form of a loop (see Fig. 4). The largest local values of heat flux far beyond $q_{\mathrm{cr},1}$ are reached in the region under the vapor bubble at the initial stage of its growth. The smallest values of heat flux are reached in the heated liquid region before bubble initiation or on dry spots if the latter appear.

This work was supported by the Russian Foundation for Fundamental Research (Grant No. 98-02-17588).

REFERENCES

1. B. P. Avksentyuk, G. I. Bobrovich, S. S. Kutateladze, and V. N. Moskvicheva, "Degeneration of bubble boiling under free convection conditions," *Prikl. Mekh. Tekh. Fiz.*, **1**, 69–73 (1972).
2. B. P. Avksentyuk and N. N. Mamontova, "Characteristics of heat-transfer crisis during boiling of alkali metals and organic fluids under free convection conditions at reduced pressure," in: *Progress in Heat and Mass Transfer*, Vol. 7, Pergamon Press, Oxford (1973), pp. 355–362.
3. B. P. Avksentyuk, V. V. Ovchinnikov, and V. Ya. Plotnikov, "Self-sustaining boiling front and a third boiling crisis," in: *Nonstationary Processes in Two-Phase Flows* [in Russian], Inst. of Thermal Phys., Novosibirsk (1989), pp. 52–68.
4. B. P. Avksentyuk and S. S. Kutateladze, "Instability of heat transfer on surfaces depleted with vaporization centers," *Teplofiz. Vys. Temp.*, **15**, No. 1, 115–120 (1977).
5. B. P. Avksentyuk, "On heat-transfer crises during boiling under free convection conditions," in: *Thermal Physics and Hydrodynamics of Boiling and Condensation* [in Russian], Inst. of Thermal Phys., Novosibirsk (1985), pp. 148–159.
6. V. M. Borishanskiy and B. S. Fokin, "Onset of heat-transfer crisis with unsteady increase in heat flux," *Heat Transfer. Sov. Res.*, **1**, No. 5, 27–55 (1969).
7. H. A. Johnson, "Transient boiling heat transfer to water," *Int. J. Heat Mass Transfer*, **14**, 67–82 (1971).
8. V. I. Tolubinskii, *Boiling Heat Transfer* [in Russian], Naukova Dumka, Kiev (1980).
9. P. A. Pavlov, *Boiling Dynamics of Strongly Superheated Liquids* [in Russian], Izd. Ural. Otd. Akad. Nauk. SSSR, Sverdlovsk (1988).
10. K. Okuyama, Y. Kozawa, A. Inoue, and S. Aoki, "Transient boiling heat transfer characteristics of R113 at large stepwise power generation," *Int. J. Heat Mass Transfer*, **51**, 2161–2174 (1988).
11. B. P. Avksentyuk and V. V. Ovchinnikov, "Dynamics of explosive boiling of toluene at subatmospheric pressures," *Teplofiz. Vys. Temp.*, **17**, No. 4, 606–613 (1999).
12. J. E. Shepherd and B. Sturtevant, "Rapid evaporation at the superheat limit," *J. Fluid Mech.*, **121**, 379–402 (1982).
13. B. P. Avksentyuk, V. V. Ovchinnikov, and V. Ya. Plotnikov, "Boiling dynamics of liquids at high superheats," in: *Heat Transfer in Steam Generators*, Materials of the All-Union Conference (Novosibirsk, June 28–30, 1988), Inst. of Thermal Phys., Novosibirsk (1988), pp. 304–308.